Extended Data Figure 1.

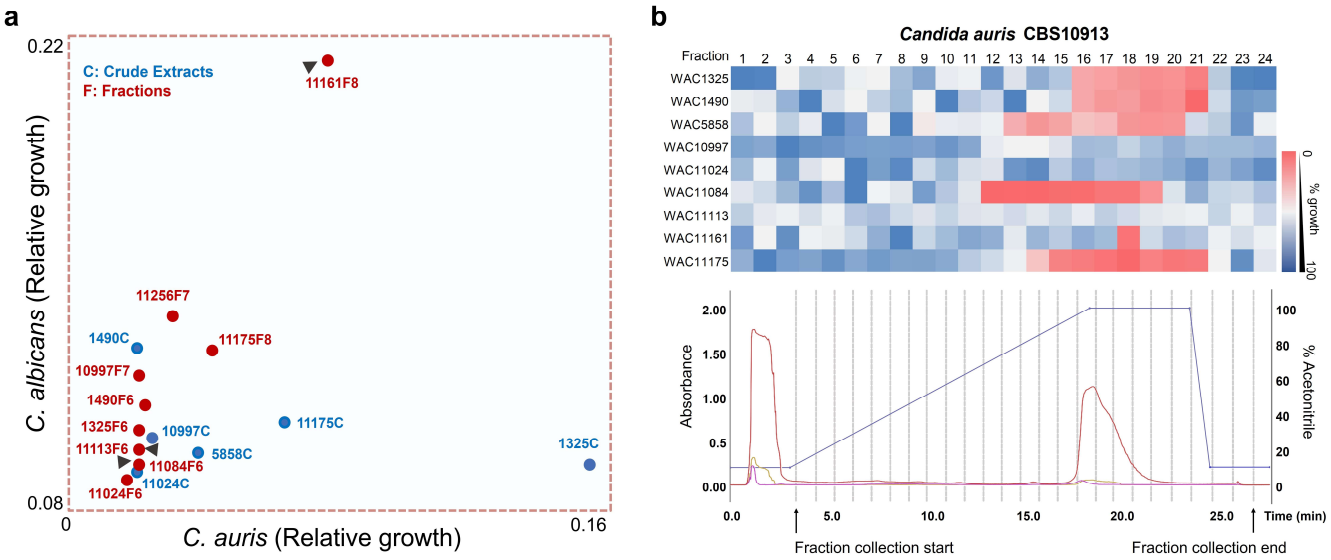

Extended Data Fig. 1| Verification of Screening Hits

a, A magnified view of the hits from high-throughput screening of the crude methanolic extracts and prefractionated library (PFL) against *C. albicans* ATCC90028 and *C. auris* CBS10913. Red circles denote hits from fractions (F), while blue circles represent hits from crude extracts (C). The corresponding WAC identity and fraction numbers are shown next to each hit. Black arrows highlight hits unique to the PFL screen. Screening results against *C. auris* and *C. albicans* are plotted on the x-axis and y-axis, respectively, showing the relative growth of *Candida* in the presence of crude extracts or fractions compared to the untreated control. **b**, Overview of validation methods and results for screening hits. The bottom panel illustrates the chromatography method, a representative Combiflash run with fraction collection events for one of the hits, WAC11175. The gradient, shown as the percentage of acetonitrile, is indicated in blue, while UV absorbance traces are displayed at 210 nm (red), 254 nm (yellow), and 280 nm (pink). The top panel presents the average growth of *C. auris* in the presence of each fraction separated as shown in the bottom panel. Biological duplicates were averaged and normalized to no-compound controls. Relative growth is represented by color (refer to the scale bar at the bottom right).

Extended Data Figure 2.

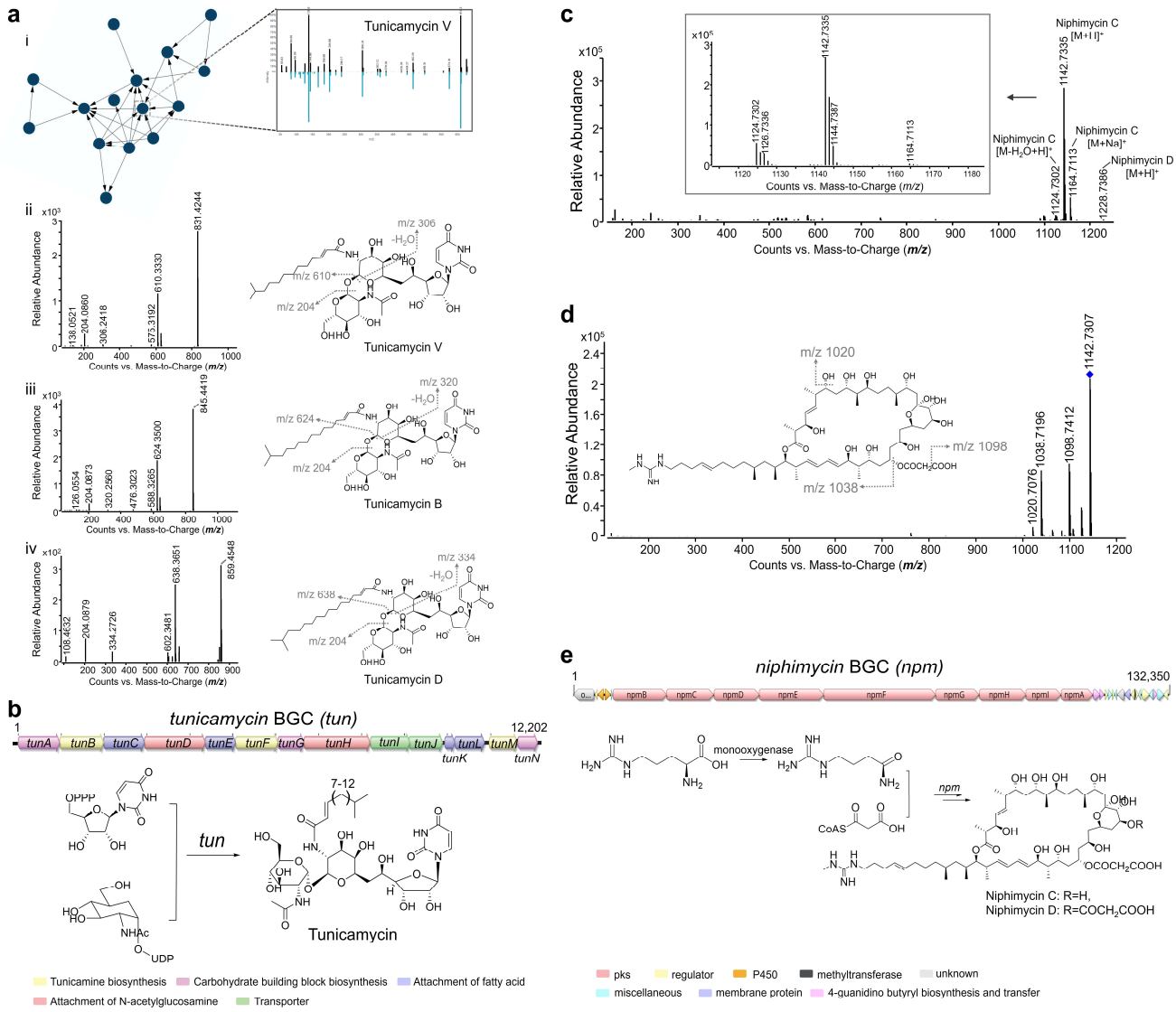

Extended Data Fig. 2| Rapid identification of known chemical scaffolds using high-resolution (HR) mass spectrometry coupled with bioinformatics analysis.

a, Identification of tunicamycins from the antifungal fractions of WAC1490. (i) GNPS molecular networking, constructed via HR-MS/MS, includes tandem MS fragment ion matches (inset panel) between the identified entity from the fractions (blue) and reference tunicamycin V (black) as an example. (ii-iv) MS/MS fragmentation patterns and structures of tunicamycins: Tunicamycin V ([M + H]+, *m/z* 831.4244) fragments into main ions at 610.3, 306.2, 204.1, etc; Tunicamycin B ([M + H]+, *m/z* 845.4419) fragments into main ions at 642.4, 624.35, 588.3, etc; Tunicamycin D ([M + H]+, *m/z* 859.4548) fragments into main ions at 638.3, 602.3, 334.3, etc. **b**, Genetic organization of the tunicamycin BGC in WAC1490 and WAC1325 and the proposed biosynthesis. Color coding indicates functional pathways: purple represents carbohydrate building block

biosynthesis; yellow, tunicamine biosynthesis; blue, fatty acid attachment; red, N-acetylglucosamine attachment; and green, transporter genes. Annotation for each gene in the biosynthetic gene clusters is provided in Supplementary Table 1. **c**, Representative HR-LCMS mass spectrum of the active fractions in WAC5858. The H^+ and Na^+ adducts of niphimycin C, along with small amounts of the H^+ adduct of niphimycin D, were identified. Niphimycin C: HRMS m/z 1142.7335 $[M + H]^+$ (calculated for $C_{59}H_{104}N_3O_{18}$, 1142.7309) and 1164.7113 $[M + Na]^+$ (calculated for $C_{59}H_{103}N_3O_{18}Na$, 1164.7129). Niphimycin D: HRMS m/z 1228.7386 $[M + H]^+$ (calculated for $C_{62}H_{106}N_3O_{21}$, 1228.7313). **d**, HRMS/MS spectrum of niphimycin C. The HRMS/MS spectrum of niphimycin C was obtained using a QToF-LCMS with flow injection at a collision energy of 50 eV. The structure of niphimycin C, along with its fragmented structure and corresponding masses, is presented. **e**, Genetic organization of the niphimycin BGC in WAC5858 genome and the proposed biosynthesis. Nine large genes (*npmA-npmI*) encode a 20-module type I polyketide synthase (PKS) responsible for assembling the polyketide skeleton of niphimycin, indicated in light red. The final structures of niphimycin C and niphimycin D are shown on the right. Color coding indicates functional genes, as depicted at the bottom. Annotated information for each gene in the biosynthetic gene cluster is available in Supplementary Table 1.

Extended Data Figure 3.

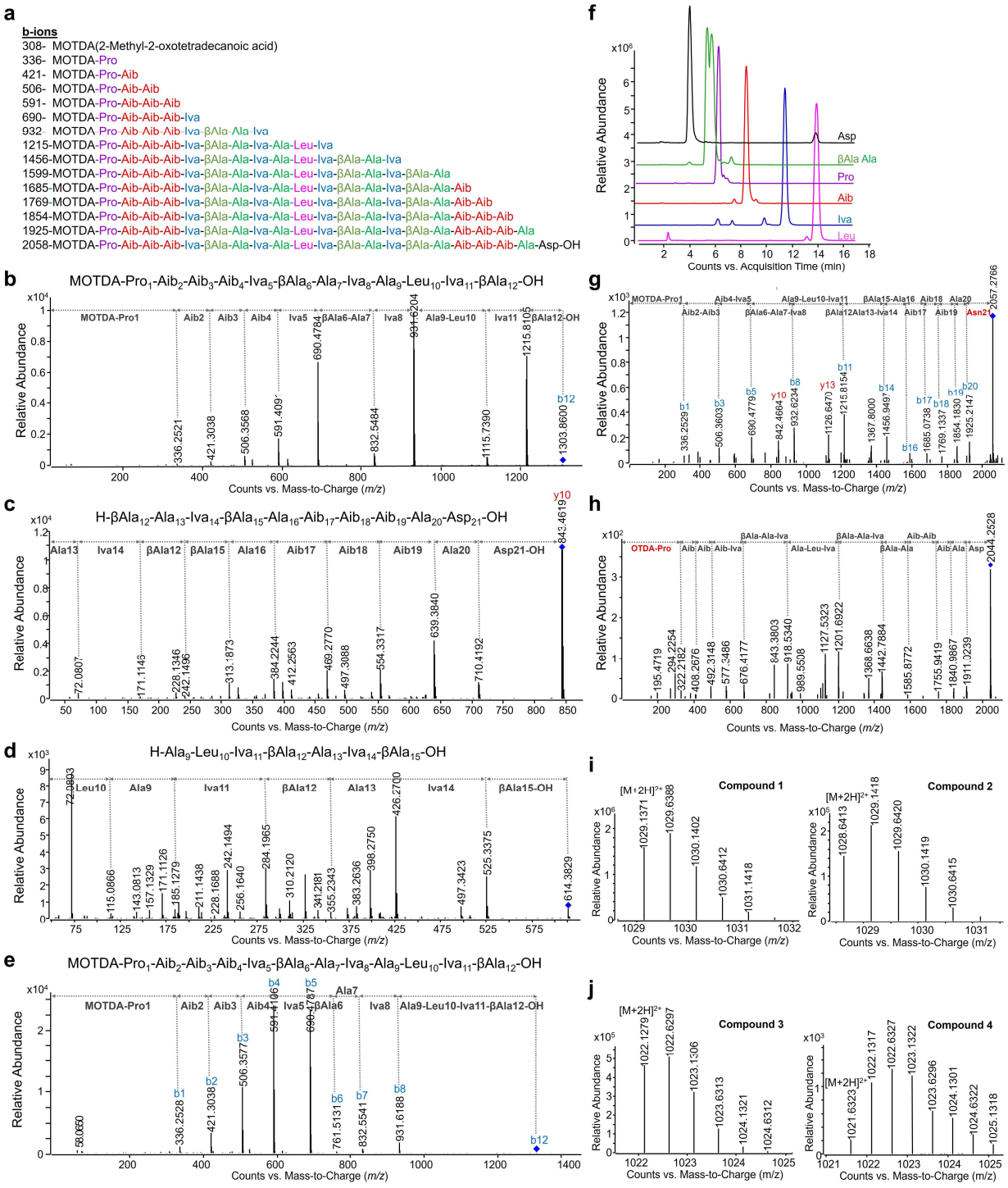

Extended Data Fig. 3| Characterization of novel antifungal lipopeptides from the *Coniochaeta* fungus WAC11161.

a, Summary of the b ion masses and their corresponding lipopeptide sequences, with color coding based on amino acids, aligned with Marfey's analysis (Extended Data Fig. 3f). **b**, MS/MS analysis

of the partially hydrolyzed product of **1** was performed using collision-induced dissociation (CID) with a product ion scan targeting the nominal *m/z* 1303.86. The precursor ion is marked with a blue square. The sequence of the lipopeptide fragment is shown above, with collision-induced fragmentation patterns displayed in the mass-loss regions of the MS/MS spectrum. The b ions are highlighted in blue. **c**, MS/MS analysis of the partially hydrolyzed product of **1** was performed using CID with a product ion scan targeting the nominal m/z 843.46. The precursor ion is marked with a blue square. The sequence of the lipopeptide fragment is shown above, with collision-induced fragmentation patterns displayed in the mass-loss regions of the MS/MS spectrum. The y ions are highlighted in red. **d**, MS/MS analysis of the partially hydrolyzed intermediate fragment of **1** was conducted using CID with a product ion scan targeting the nominal *m/z* 614.38. The precursor ion is marked with a blue square. The sequence of the lipopeptide fragment is shown above, with collision-induced fragmentation patterns displayed in the mass-loss regions of the MS/MS spectrum. **e**, MS/MS analysis of the partially hydrolyzed product of **1** was performed using CID with a product ion scan targeting the nominal *m/z* 1303.86. The analysis is identical to Extended Data Fig. 3b, but with the CID energy increased to 50 eV to achieve sequence resolution at the single-residue level. **f**, Marfey's analysis of **1** was performed, involving HPLC separation of the modified, hydrolyzed peptide. The analysis revealed seven amino acids in **1**: α-amino-iso-butyric acid (Aib), D-iso-valine (Iva), β-Alanine (βAla), L-Alanine (Ala), L-Leucine (Leu), L-Proline (Pro), and L-Aspartic acid (Asp). **g**, MS/MS analysis of **2** was performed using CID with a product ion scan targeting the nominal m/z 2056.27. The precursor ion is indicated with a blue square. The collision-induced fragmentation pattern is displayed in the mass-loss regions of the MS/MS spectrum with b ions labeled in blue, and the y ions labeled in red. The C-terminal asparagine (Asn) is highlighted in red. **h**, MS/MS analysis of **3** was conducted using collision-induced dissociation (CID) with a product ion scan targeting the nominal *m/z* 2043.24. The precursor ion is marked with a blue square. The collision-induced fragmentation pattern is shown in the mass-loss regions of the MS/MS spectrum, with the N-terminal 3-oxotetradecanoic acid (OTDA) highlighted in red. **i**, High-resolution mass spectra of **1** and **2** obtained using QToF mass spectrometry, showing the $[M+2H]^{2+}$ ions at m/z 1029.1371 and 1028.6413, respectively. **j**, High-resolution mass spectra of **3** and **4** obtained using QToF mass spectrometry, showing the $[M+2H]^{2+}$ ions at m/z 1022.1279 and 1021.6323, respectively.

Extended Data Figure 4.

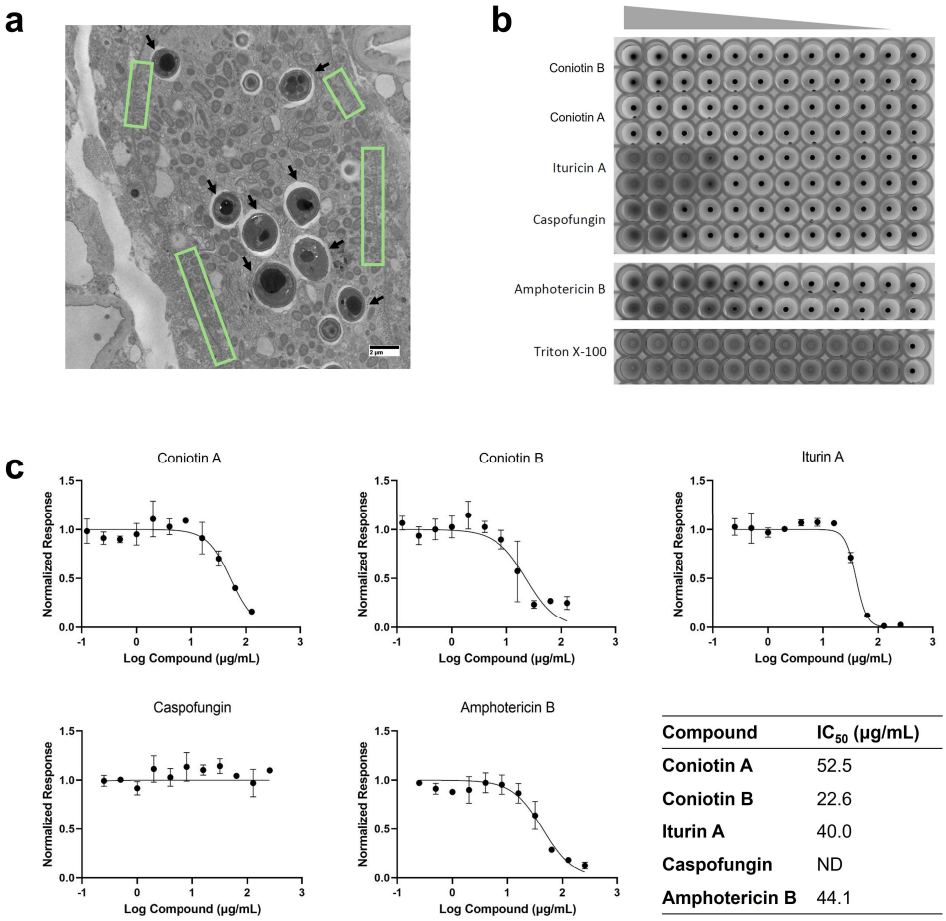

Compound	IC_{50} (µg/mL)
Coniotin A	52.5
Coniotin B	22.6
Iturin A	40.0
Caspofungin	ND
Amphotericin B	44.1

Extended Data Fig. 4| Therapeutic potential assessment of coniotins.

a, TEM images of the *C. elegans* intestine infected with *C. auris*. Black arrows indicate *C. auris* CBS12775 cells. Green boxes highlight the disintegration of the brush border in the gastrointestinal tract. The image is taken from longitudinal sections of *C. elegans*. Scale bar = 2 µm. **b**, Hemolysis data. An 11-point dose-response series was prepared for the compounds, using two-fold dilutions. The starting concentration was 128 µg/mL for coniotin A and B, and 256 µg/mL for iturin A, caspofungin, and amphotericin B. Triton X-100, starting at 20%, served as the positive control. Hemolysis was identified by the presence of red supernatant in the wells. A DMSO-only control was included in the last column of each row. **c**, Cytotoxicity assessment of coniotin A, coniotin B, caspofungin, amphotericin B, and iturin A. HEK293 cells were used for the evaluation. IC50 curves were generated using 11-point dose-response curves with two-fold dilutions for each compound. Luminescence values were normalized to the DMSO control. The starting concentration was 128 µg/mL for coniotin A and B, and 256 µg/mL for iturin A, caspofungin, and amphotericin B. The IC50 values are presented in the table below.

Extended Data Figure 5.

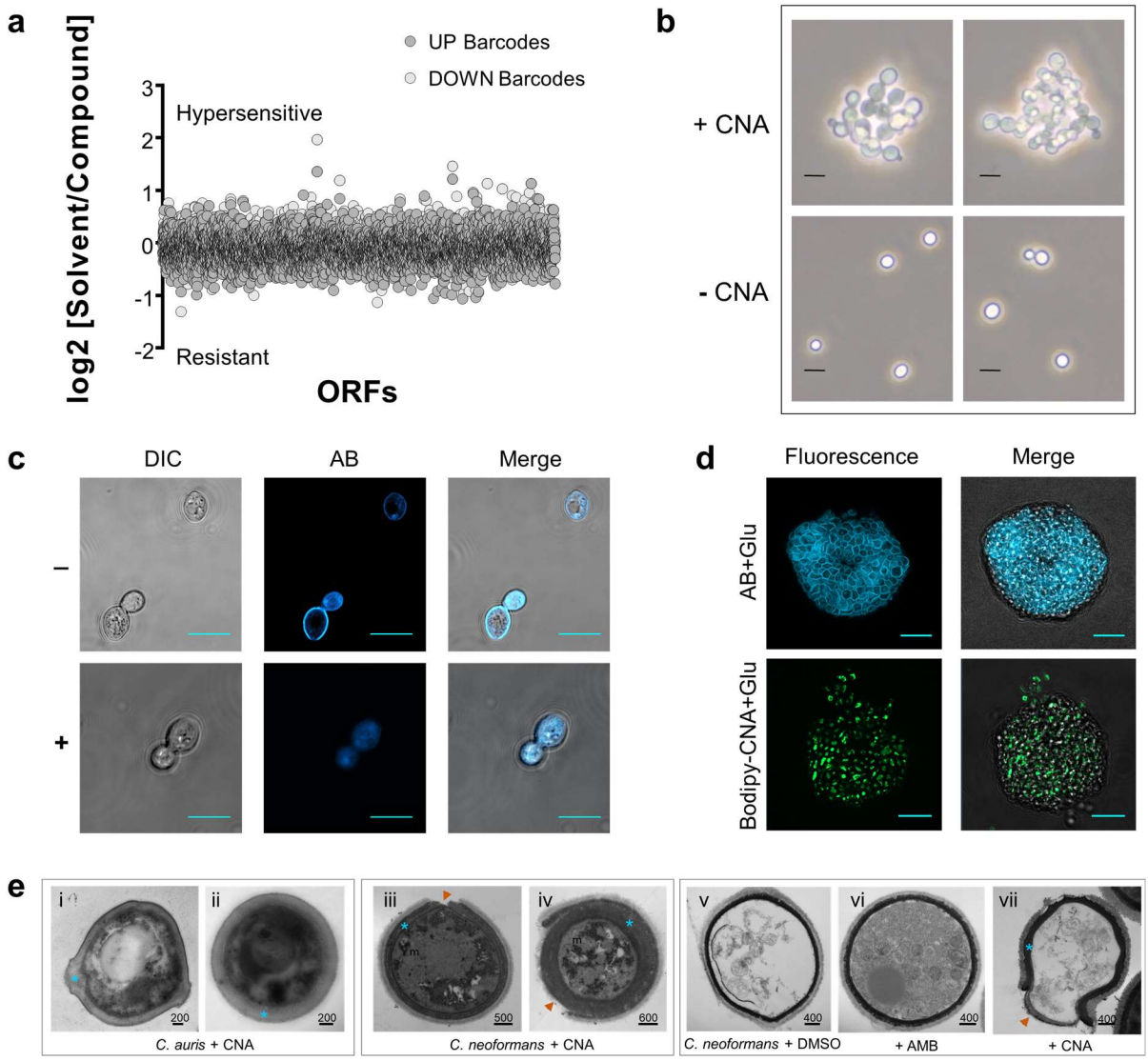

Extended Data Fig. 5| Coniotin A specifically targets β-glucan impairing cell wall integrity.

a, Haploinsufficiency profiling (HIP) analysis was performed using a pooled library of double-barcoded heterozygous *C. albicans* deletion mutants grown in YPD medium with or without sub-inhibitory concentrations of coniotin A (10 or 14 µg/mL, causing 10–50% growth inhibition). The relative abundance of each strain was determined by high-throughput sequencing of two strain-specific barcodes (UP-TAG and DN-TAG). Gray dots represent strains not identified as hits, as neither barcode showed a log2 fold-change greater than 2. **b**, Light micrographs of *C. albicans* ATCC 90028 illustrating the impact of coniotin A (CNA) on fungal morphogenesis. Cultures were treated with 2 µg/mL CNA (+) or left untreated (-) in SDB media, and cellular morphology was visualized using an EVOS FL Auto microscope at 40× magnification. Scale bar: 5 µm. **c**, Aniline blue (AB) staining analysis of the β-1,3-glucan layer in the cell wall of *C. albicans* ATCC90028,

with (+) and without (-) treatment using 1 μg/mL coniotin A. Images were acquired using a Zeiss LSM 980 Upright Confocal Microscope using a 63×/1.4 oil-immersion objective. DIC: differential interference contrast (brightfield microscopic image); AB: aniline blue fluorescence image; Merge: overlay of DIC and AB images. Scale bar = 5 μm. **d**, Confocal fluorescence microscopy images of β-1,3-glucan (Glu) incubated with 120 μM BODIPY-conjugated coniotin A (BODIPY-CNA) for 1 hour in PBS, followed by three washes before visualization using a Zeiss LSM 980 Upright Confocal Microscope. Aniline blue (AB) staining was used to analyze the β-1,3-glucan particles. Fluorescence images are shown separately as fluorescence channels, with "Merge" representing an overlay of the brightfield and fluorescence images. Scale bar = 10 μm. **e**, Additional TEM images of *C. auris* CBS12766 and *C. neoformans* H99 reveal abnormal cell wall structures after coniotin A (CNA) treatment (refer to Fig. 5j). CNA-treated *C. auris* cells are shown in (i, ii), CNA-treated *C. neoformans* in (iii, iv, vii), and amphotericin B (AMB)-treated and untreated *C. neoformans* dead cells in (vi, v). Observed cell wall defects in CNA-treated cells include multilayered cell walls and focal enlargements (blue asterisks), compromised cell wall integrity (orange arrowheads), and abnormally increased thickness. Scale bars are depicted in each image, with units in nanometers (nm).